

Bulk-sensitive photoemission spectroscopy of $A_2\text{FeMoO}_6$ double perovskites ($A = \text{Sr}, \text{Ba}$)J.-S. Kang,¹ J. H. Kim,¹ A. Sekiyama,² S. Kasai,² S. Suga,² S. W. Han,³ K. H. Kim,³ T. Muro,⁴ Y. Saitoh,⁵ C. Hwang,⁶ C. G. Olson,⁷ B. J. Park,⁸ B. W. Lee,⁸ J. H. Shim,⁹ J. H. Park,⁹ and B. I. Min⁹¹Department of Physics, The Catholic University of Korea, Puchon 420-743, Korea²Department of Material Physics, Graduate School of Engineering Science, Osaka University, Osaka 560-8531, Japan³Department of Physics, Gyeongsang National University, Chinju 660-701, Korea⁴Japan Synchrotron Radiation Research Institute (JASRI), SPring-8, Hyogo 679-5198, Japan⁵Department of Synchrotron Radiation Research, Kansai Research Establishment, Japan Atomic Energy Research Institute (JAERI), SPring-8, Hyogo 679-5148, Japan⁶Korea Research Institute of Standards and Science, Taejeon 305-600, Korea⁷Ames Laboratory, Iowa State University, Ames, Iowa 50011, U.S.A.⁸Department of Physics, Hankuk University of Foreign Studies, Yongin, Kyungki 449-791, Korea⁹Department of Physics, Pohang University of Science and Technology, Pohang 790-784, Korea

(Received 8 July 2002; published 30 September 2002)

The electronic structures of $\text{Sr}_2\text{FeMoO}_6$ (SFMO) and $\text{Ba}_2\text{FeMoO}_6$ (BFMO) double perovskites have been investigated using Fe $2p \rightarrow 3d$ resonant photoemission spectroscopy (PES) and the Cooper minimum in the Mo $4d$ photoionization cross section. The states close to the Fermi level are found to have a strongly mixed Mo-Fe t_{2g} character, indicating that the Fe valence is far from pure $3+$. The Fe $2p_{3/2}$ x-ray absorption spectroscopy spectra reveal the mixed-valent Fe^{3+} - Fe^{2+} configurations, and a larger Fe^{2+} component for BFMO than for SFMO, suggesting an operative double exchange interaction. The valence-band PES spectra reveal good agreement with the local-spin-density-approximation (LSDA)+ U calculation.

DOI: 10.1103/PhysRevB.66.113105

PACS number(s): 75.70.Pa, 71.30.+h, 79.60.-i

Room-temperature magnetoresistance (MR) has recently been observed in the double-perovskite oxides of $A_2BB'\text{MoO}_6$ ($A = \text{Sr}, \text{Ba}$; $B = \text{Fe}, B' = \text{Mo}$) with very high magnetic transition temperatures T_C (≈ 330 – 450 K).¹⁻³ A fundamental question in the double perovskites is the origin of the high- T_C ferrimagnetism and the low field MR. Magnetization data for $\text{Sr}_2\text{FeMoO}_6$ (SFMO) indicated ferrimagnetic coupling between Fe^{3+} and Mo^{5+} ions,⁴ and the MR was interpreted as due to intergrain tunneling with the half-metallic electronic structure.^{1,5,6} Neutron diffraction and Mössbauer spectroscopy on $A_2\text{FeMoO}_6$ indicated an Fe moment of $(4.0$ – $4.1)\mu_B$ but a rather small localized moment on Mo, $(-0.2$ – $-0.5)\mu_B$.^{2,7,8} The ferrimagnetic coupling between Fe^{3+} and Mo^{5+} can be understood in terms of the superexchange through the Fe-O-Mo π bonding. The superexchange model, however, is not compatible with the metallic nature of SFMO and $\text{Ba}_2\text{FeMoO}_6$ (BFMO). Further, the valence states of Fe and Mo ions are still controversial; some works were interpreted the value of Fe^{3+} ,^{1,9} while other works favored the mixed valence of Fe^{3+} - Fe^{2+} .^{7,10,11}

Photoemission spectroscopy (PES) can provide direct information on the electronic structures of the double perovskites, but no valence-band PES study on SFMO has been reported so far^{12,13} to our knowledge. In this paper, we report a *bulk-sensitive*¹⁴ high-resolution valence-band PES study for SFMO and BFMO, including resonant photoemission spectroscopy (RPES) near the Fe $2p$ absorption edge and the O $1s$ and Fe $2p$ x-ray absorption spectroscopy (XAS) measurements.

Polycrystalline SFMO and BFMO samples were prepared by the standard solid-state reaction method.¹² The measured saturation magnetic moments are larger than $3.8\mu_B$ (BFMO) and $3.4\mu_B$ (SFMO) per formula unit (f.u.), reflecting the well ordered Fe and Mo ions at B and B' sites. High-resolution Fe

$2p \rightarrow 3d$ RPES experiments were performed at the twin-helical undulator beam line BL25SU of SPring-8 equipped with a SCIENTA SES200 analyzer.¹⁵ Samples were fractured and measured in vacuum better than 3×10^{-10} Torr at $T \leq 20$ K. PES data were obtained in the angle-integrated mode, and the Fermi level E_F and overall energy resolution of the system were determined from the Fermi-edge spectrum of Pd metal. The total instrumental resolution (FWHM: full width at half maximum) was about 130 meV at $h\nu \sim 700$ eV. All the spectra were normalized to the photon flux estimated from the mirror current. Both samples showed a clean single peak in the O $1s$ core-level spectrum, and no 9-eV binding energy (BE) peak in the valence-band spectrum (see Fig. 2). Low energy PES experiments were carried out at the Ames/Montana beamline at the Synchrotron Radiation Center in a vacuum better than 3×10^{-11} Torr.¹² The fractured surfaces were rough and the measured spectra showed no angle dependence, suggesting that our PES data could be considered as being angle integrated.

Figure 1 shows the RPES valence-band spectra of SFMO and BFMO near the Fe $2p_{3/2}$ absorption edge. The top panels show the measured Fe $2p_{3/2}$ XAS spectra (left) and the calculated XAS spectra (right). The arrows in the XAS spectra represent $h\nu$'s where the spectra are obtained. For both SFMO and BFMO, the features near E_F (~ -0.3 eV), at ~ -1.5 , -3 , and -4 eV in the valence-band spectra are enhanced greatly across the Fe $2p$ absorption edge, indicating that these states have large Fe $3d$ character. As to the resonating behavior, the Fe $3d$ -derived states at -0.3 and -1.5 eV are due to the $t_{2g}^x \downarrow$ and $e_g^2 \uparrow$ states, respectively ($0 < x \leq 1$).¹² These RPES measurements reveal that the high BE features ($-3 \sim -8$ eV) also have the substantially large Fe $3d$ electron character, which is strongly hybridized with

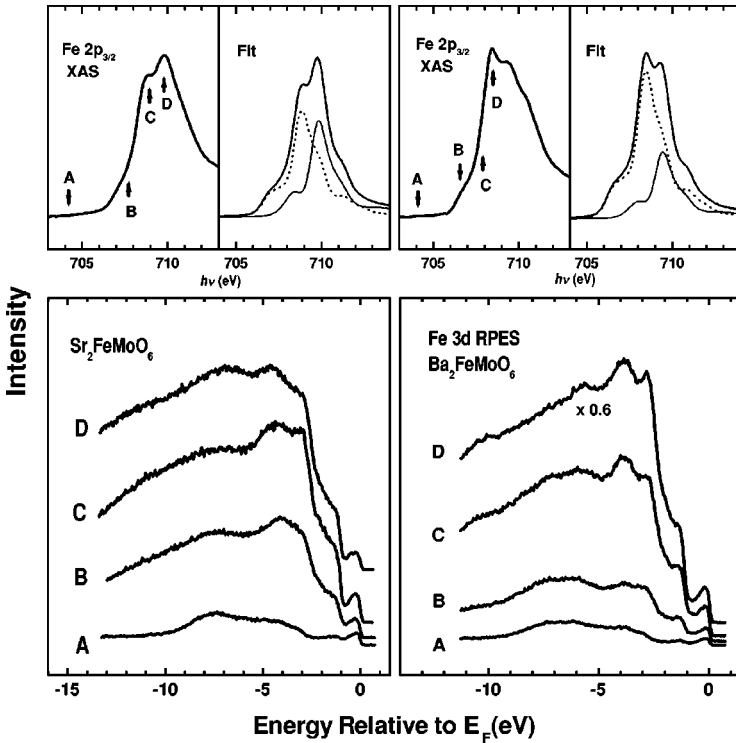


FIG. 1. Top: the measured Fe $2p_{3/2}$ XAS spectra (left) and the fitting results (right) for SFMO and BFMO. In the calculated XAS spectra (right), dotted lines, gray lines, and solid lines denote the Fe²⁺ and Fe³⁺ components, and their sum, respectively. Bottom: valence-band spectra of SFMO and BFMO near the Fe $2p \rightarrow 3d$ absorption edge.

the O $2p$ electrons. In the above $h\nu$ region, however, the features for $E \lesssim -5$ eV are obscured by the overlapping broad Fe LMM Auger emission, which is evident as the non-flat slope for $E \lesssim -8$ eV for $h\nu \gtrsim 708$ eV.

Our Fe $2p_{3/2}$ XAS spectrum for SFMO is basically similar to those of previous reports.^{9,16} But the shoulder around $h\nu \sim 707$ eV in the low- $h\nu$ side of the main $2p_{3/2}$ XAS peak, clearly observed in our XAS spectra of both SFMO and BFMO, is not observed in the previous data in the literature,^{9,16} which is due to the better resolution (~ 100 meV) employed in our XAS spectra. It is evident that the relative intensities between the two peaks of the $2p_{3/2}$ absorption maxima ($h\nu \approx 708$ and 710 eV) are reversed in SFMO and BFMO; namely, a stronger peak is located at a higher $h\nu$ for SFMO but at a lower $h\nu$ for BFMO. We believe that this difference is intrinsic since both samples showed a clean single peak in the O $1s$ spectrum, and essentially the same XAS spectrum was reproduced with different fractures. It has been known that the $2p_{3/2}$ absorption edge of Fe²⁺ ions in the octahedral symmetry exhibits a main peak at a lower $h\nu$ than that of Fe³⁺ ions.^{17,18} Thus the difference in the Fe $2p_{3/2}$ XAS spectra between SFMO and BFMO suggests that Fe ions in BFMO have a larger 2+ component than in SFMO. One possible reason for such a difference might be the different oxygen relaxation between Fe and Mo due to different ion radii of Ba and Sr ions. Indeed, the structural data provide that the relative Fe-O bond length is smaller in SFMO, so as to have a higher Fe valence state than in BFMO.^{8,19}

In order to estimate the Fe valences of SFMO and BFMO in the ground states, we have analyzed the XAS spectra of SFMO and BFMO within the configuration interaction cluster model where the effects of the multiplet interaction, the crystal field, and the hybridization with the O p ligands are

included.^{20,21} In this analysis, we have considered two configurations, d^n and $d^{n+1}L^1$ (L is a ligand hole), since the $d^{n+2}L^2$ configuration gives negligible effect. In the calculation of the Fe²⁺ ($n=6$) and Fe³⁺ ($n=5$) XAS spectra, we have used the same parameters as used for FeO and α -Fe₂O₃, respectively.¹⁸ We have checked that small changes in the parameters do not affect the overall spectral shape including the prominent peak positions. The calculated XAS spectra (the top-right panels) reveal that the ground states of both SFMO and BFMO are strongly mixed valent, with Fe²⁺ and Fe³⁺ configurations. The estimated Fe valences are about 2.5 for SFMO and 2.3 for BFMO. If we use the Fe³⁺ component only (d^5 and d^6L^1), the experimental features of the reversed XAS line shape for BFMO and the low- $h\nu$ shoulders ($h\nu \sim 707$ eV) cannot be reproduced.

Figure 2 compares the valence-band spectra of SFMO and BFMO for a wide $h\nu$ range ($22 \text{ eV} \leq h\nu \leq 700 \text{ eV}$). The top two spectra are the differences between the on-resonance ($h\nu \approx 708$ eV) and off-resonance spectra in the Fe $2p \rightarrow 3d$ RPES, which can be considered as representing the Fe $3d$ partial spectral weight (PSW) distributions. If one assumes Fe³⁺ ($3d^5$), Mo⁵⁺ ($4d^1$), and the filled O $2p$ bands ($2p^6$) in AFMO, then the cross-section ratio of Fe $3d$: Mo $4d$: O $2p$ per unit cell is about $\sim 4\%$: $\sim 5\%$: $\sim 91\%$ at $h\nu \approx 20$ eV, $\sim 25\%$: $\sim 0\%$: $\sim 75\%$ at $h\nu \approx 90$ eV, and $\sim 41\%$: $\sim 9\%$: $\sim 49\%$ at $h\nu \approx 700$ eV.²² The $h\nu = 22$ eV spectrum can be considered as the O $2p$ PSW. With increasing $h\nu$, the Fe $3d$ and Mo $4d$ emissions increase with respect to the O $2p$ emission, except for the $h\nu$ region corresponding to the Cooper minimum in the Mo $4d$ cross section around $h\nu \sim 90$ eV, and the Fe $3d$ and O $2p$ emissions become comparable at $h\nu \approx 700$ eV. Consequently, the Mo $4d$ emission is negligible at $h\nu \sim 90$ eV, and becomes the largest in the Fe

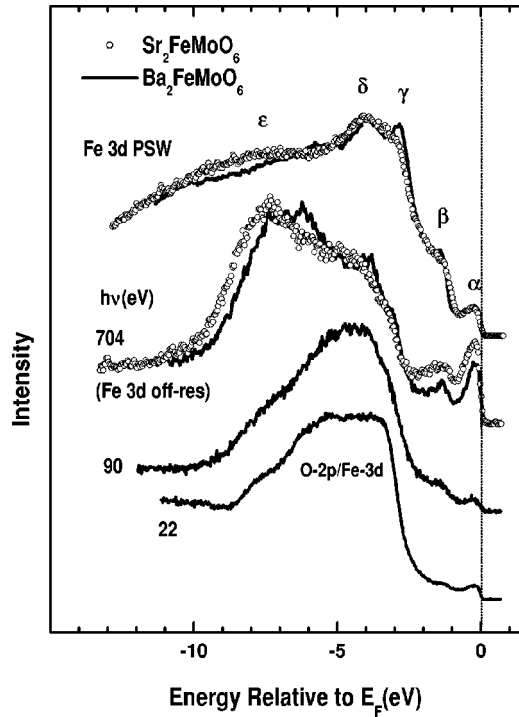


FIG. 2. Comparison of the valence-band spectra of SFMO (dots) and BFMO (solid lines) for a wide $h\nu$ range.

$3d$ off-resonance spectrum ($h\nu=704$ eV). Thus the pronounced feature at E_F at $h\nu=704$ eV is due to the larger Mo $4d$ contribution, and may also represent the intrinsic bulk feature, compared to the cases at low $h\nu$'s.^{14,23}

The valence-band spectra of SFMO and BFMO share very common features. First, metallic Fermi edges are observed in both systems at $T\sim 20$ K, which confirms the metallic behavior at low T . Second, several structures appear at similar energies, labeled as α (-0.3 eV), β (-1.5 eV), γ (-3.5 eV), δ (-4 eV), and ϵ (~ -8 eV). Based on the finding in Fig. 1, the features of α, β, γ , and δ are identified to have a large Fe $3d$ -derived electron character. Note that the peak α is much larger at $h\nu=704$ eV than at $h\nu=90$ eV (Cooper minimum), showing that the peak α has predominant Mo $4d$ electron character. Therefore, the peak α has both Mo $4d$ and Fe $3d$ electron character.

We now discuss the differences in the valence-band spectra between SFMO and BFMO. First, the α peak at E_F for BFMO is weaker than that in SFMO at $h\nu=704$ eV. Considering that the intensity of the peak α is very similar for SFMO and BFMO in the Fe $3d$ PSW's (top curves), this difference implies that the Mo $4d$ electron occupancy in BFMO is lower than that in SFMO. Accordingly, this finding indicates larger Fe²⁺–Mo⁶⁺ character in BFMO than in SFMO, which is consistent with that of the Fe $2p_{3/2}$ XAS spectra (Fig. 1). Secondly, the band width of the O $2p$ –Fe $3d$ peak in BFMO is narrower than that in SFMO. This difference is in agreement with the local spin density approximation (LSDA)+ U (U : the Coulomb correlation parameter) calculations shown in Fig. 3, and reflects the larger Fe–O–Mo bond length in BFMO due to its larger lattice constant.¹⁹

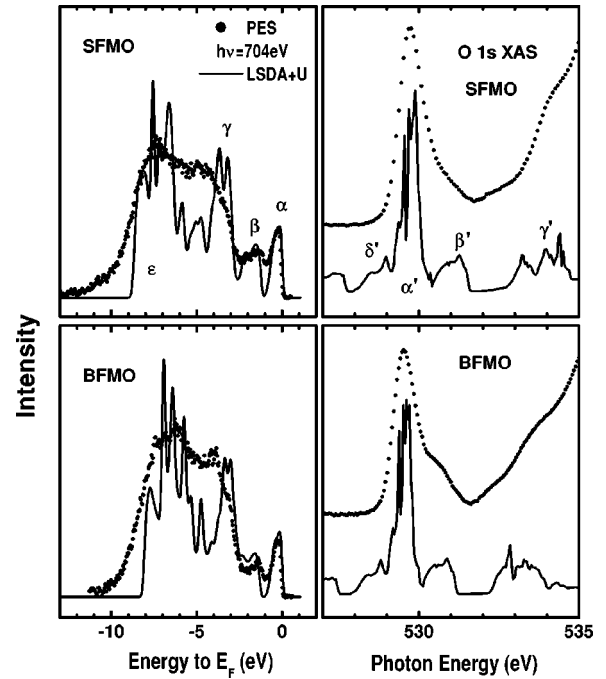


FIG. 3. Left: comparison of the $h\nu=704$ eV valence-band spectra (dots) to the weighted sum of the PLDOS's (solid lines) obtained from the LSDA+ U calculation. α : Mo $t_{2g\downarrow}$ –Fe $t_{2g\downarrow}$ hybridized states; β : Fe $e_g\uparrow$, γ : Fe $t_{2g\uparrow}$; ϵ : Mo $4d$ –Fe $3d$ –O p hybridized bonding states. Right: comparison of the O $1s$ XAS spectra to the sum of the Fe $3d$, Mo $4d$, O $2p$, and Sr(Ba) s/p PLDOS's. α' : Mo $t_{2g\uparrow}$ and Fe $t_{2g\downarrow}$ character; β' : Fe $e_g\downarrow$; γ' : Mo $e_g\uparrow\downarrow$; δ' : Mo $t_{2g\downarrow}$.

The left panel of Fig. 3 compares the $h\nu=704$ eV valence-band spectra (dots) to the weighted sum of the PLDOS's (projected local densities of states) of Fe $3d$, Mo $4d$, and O $2p$ states (solid lines). The PLDOS's have been obtained from the LSDA+ U calculation.¹² The parameters used in this calculation are $U=3.0$ eV and $J=0.97$ eV (J is the exchange correlation parameter) for Fe $3d$ electrons.²⁴ For the comparison to the valence-band spectra, the summed PLDOS's below E_F have been convoluted with a Gaussian function of 0.2 eV at the FWHM to simulate the instrumental resolution. The right panel compares the O $1s$ XAS spectra to the sum of the unoccupied part of the Fe $3d$, Mo $4d$, O $2p$, and Sr (Ba) s/p PLDOS's. The O $1s$ XAS spectrum reflects the transition from the O $1s$ to the unoccupied O $2p$ states hybridized to the other electronic states, and so it provides a reasonable approximation for representing the unoccupied conduction bands.

The LSDA+ U calculations agree quite well with the valence-band spectra, in the peak positions and the bandwidths, and also explain the low energy features of the XAS spectra reasonably well. If we shift the O $1s$ XAS spectra by referring to the LSDA+ U calculations,^{12,25} the energy separations between the lowest energy peaks in the valence-band PES (α) and those in the O $1s$ XAS (α') spectra become about ~ 1 eV. This value is comparable to, but slightly larger than, the low energy peak observed in the optical conductivity spectrum for SFMO,⁶ which was ascribed to the Fe

$e_{2g}\uparrow \rightarrow \text{Mo } t_{2g}\uparrow$ interband transition. Our finding, however, indicates that this energy separation is ascribed to the energy difference between the occupied Mo $t_{2g}\downarrow - \text{Fe } t_{2g}\downarrow$ hybridized state and the unoccupied Fe $t_{2g}\downarrow$ state mixed with O $p - \text{Mo } t_{2g}$ states.

We have found that the Fe $t_{2g}\downarrow$ and Mo $t_{2g}\downarrow$ bands are almost degenerate and t_{2g} electrons are itinerant. This suggests that two valence states $\text{Fe}^{3+} - \text{Mo}^{5+}$ and $\text{Fe}^{2+} - \text{Mo}^{6+}$ are degenerate, which would then produce a type of double exchange (DE) interaction.²⁶ That is, hopping of itinerant $t_{2g}\downarrow$ electrons between Fe and Mo sites yields a kinetic energy gain to induce ferrimagnetism between Fe and Mo spins and the half-metallicity in SFMO and BFMO. Consequently, Fe and Mo ions in SFMO and BFMO do not have definite valence states.^{10,11} The difference from the case of colossal magnetoresistant (CMR) manganites is that the spins of itinerant carriers in double perovskites are opposite to the localized Fe spins ($t_{2g}^3\uparrow e_g^2\uparrow$). Sarma *et al.*¹³ and Fang *et al.*²⁷ recently proposed alternative models to explain the magnetism in double perovskites. They regarded the double perovskite system as a ferromagnet not a ferrimagnet. That is, originally nonmagnetic Mo t_{2g} electrons are antiferromagnetically polarized by the ferromagnetically ordered Fe^{3+} spins through the hybridization between Fe $3d$ and Mo $4d$ states, thereby the resulting kinetic energy gain stabilizes the ferromagnetic state. In view of the role of kinetic energy optimization, this mechanism seems similar to the DE mechanism. However, using their models, it is hard to explain the ferrimagnetism observed in the insulating double perovskites such as $\text{Ca}_2\text{FeReO}_6$ and Ba_2BReO_6 ($B = \text{Mn, Co, Ni}$) which have one more d electron in the B' site.²⁶

Ferrimagnetism in the insulating double perovskites of $A_2BB'O_6$ is better described in terms of the superexchange

interaction through $B-B'-O$ π orbitals. In the metallic SFMO and BFMO systems, the DE-like interaction becomes operative due to the degenerate Fe and Mo $t_{2g}\downarrow$ states near E_F . In the DE mechanism, the magnetic transition temperature T_C is proportional to the hopping strength, i.e., the bandwidth of the itinerant $t_{2g}\downarrow$ states.²⁸ The observed correlation between T_C and the estimated bandwidth in metallic double perovskites provides evidence for the operation of the DE-like interaction.¹⁹ Noteworthy is that both the superexchange and the DE interactions induce the ferrimagnetism in double perovskites, differently from the case of CMR manganites in which two interactions are competitive. Further, the Jahn-Teller effect would be weaker in double perovskites due to relevant t_{2g} orbitals near E_F , as compared to e_g orbitals in manganites. Hence T_C can be high for SFMO and BFMO.

In conclusion, using the bulk-sensitive Fe $2p \rightarrow 3d$ RPES and O $1s$ XAS, the states close to E_F are found to be predominantly of Mo $t_{2g}\downarrow$ and Fe $t_{2g}\downarrow$ character, indicating that the Fe valence is far from pure $3+$ (d^5). The Fe $2p_{3/2}$ XAS spectra show that the ground states of both SFMO and BFMO consist of the strongly mixed $\text{Fe}^{3+} - \text{Fe}^{2+}$ configurations, and that BFMO has the larger Fe^{2+} component. The measured valence-band spectra agree very well with the LSDA+ U calculation. Our findings suggest that a type of DE interaction is operative in SFMO and BFMO to produce the half metallicity and ferrimagnetism.

Helpful discussions with D.D. Sarma are greatly appreciated. This work was supported by the KOSEF through the CSCMR at SNU and the eSSC at POSTECH. PES experiments were performed at the SPring-8 (JASRI: 2001B0028-NS-np) and at the SRC (NSF: DMR-0084402).

¹K.-I. Kobayashi *et al.*, Nature (London) **395**, 677 (1998).

²R.P. Borges *et al.*, J. Phys.: Condens. Matter **11**, L445 (1999).

³Y. Moritomo *et al.*, Phys. Rev. B **61**, R7827 (2000).

⁴F.S. Galasso, F.C. Douglas, and R.J. Kasper, J. Chem. Phys. **44**, 1672 (1966).

⁵T.H. Kim *et al.*, Appl. Phys. Lett. **74**, 1737 (1999).

⁶Y. Tomioka *et al.*, Phys. Rev. B **61**, 422 (2000).

⁷B. Garcia-Landa *et al.*, Solid State Commun. **110**, 435 (1999).

⁸Y. Moritomo *et al.*, Phys. Rev. B **62**, 14 224 (2000).

⁹S. Ray *et al.*, Phys. Rev. Lett. **87**, 097204 (2001).

¹⁰J. Linden *et al.*, Appl. Phys. Lett. **76**, 2925 (2000).

¹¹O. Chmaissem *et al.*, Phys. Rev. B **62**, 14 197 (2000).

¹²J.-S. Kang *et al.*, Phys. Rev. B **64**, 024429 (2001); J.-S. Kang, *et al.*, J. Phys. Soc. Jpn. Suppl. **71**, 157 (2002).

¹³D.D. Sarma *et al.*, Phys. Rev. Lett. **85**, 2549 (2000) (Mo $3d$ core-level photoemission spectroscopy study).

¹⁴Our argument of bulk sensitivity of Fe $2p \rightarrow 3d$ RPES is based on the much longer mean free paths of photoelectrons (10–20 Å) at a high excitation energy ($h\nu \sim 700$ eV), compared to those at a low excitation energy (5–10 Å at $h\nu \leq 100$ eV). Also see Ref. 23.

¹⁵Y. Saitoh *et al.*, Rev. Sci. Instrum. **71**, 3254 (2000).

¹⁶M.S. Moreno *et al.*, Solid State Commun. **120**, 161 (2001).

¹⁷G. van der Laan and I.W. Kirkman, J. Phys.: Condens. Matter **4**, 4189 (1992).

¹⁸J.P. Crocombette *et al.*, Phys. Rev. B **52**, 3143 (1995).

¹⁹C. Ritter *et al.*, J. Phys.: Condens. Matter **12**, 8295 (2000).

²⁰F.M.F. de Groot, J. Electron Spectrosc. Relat. Phenom. **67**, 529 (1994).

²¹J. H. Shim and B. I. Min (unpublished).

²²Atomic photoionization cross sections are given in J.J. Yeh and I. Lindau, At. Data Nucl. Data Tables **32**, 1 (1985).

²³A. Sekiyama *et al.*, Nature (London) **403**, 398 (2000).

²⁴Even the LSDA+ U gives the integer total magnetic moments ($4.0\mu_B$ per f. u.), reflecting the robust half-metallic nature of SFMO and BFMO.

²⁵The O $1s$ XAS spectra of SFMO and BFMO are shifted by -528.7 and -528.5 eV, respectively. There is some uncertainty in choosing the zero positions from the XAS spectra.

²⁶A.W. Sleight and J.F. Weiher, J. Phys. Chem. Solids **33**, 679 (1972).

²⁷Z. Fang, K. Terakura, and J. Kanamori, Phys. Rev. B **63**, 180407 (2001).

²⁸A. Chattopadhyay and A.J. Millis, Phys. Rev. B **64**, 024424 (2001).